Clin Exp Metastasis (2012) 29:865–877
DOI 10.1007/s10585-012-9465-5

RESEARCH PAPER

Periostin, a stroma-associated protein, correlates with tumor invasiveness and progression in nasopharyngeal carcinoma

Meixiang Li · Cui Li · Danjuan Li · Yuanjie Xie · Jinfeng Shi · Guoqing Li · Yongjun Guan · Maoyu Li · Pengfei Zhang · Fang Peng · Zhiqiang Xiao · Zhuchu Chen

Received: 17 October 2011 / Accepted: 26 February 2012 / Published online: 17 June 2012

Abstract Recently, the tumor microenvironment is increasingly recognized as playing an important role in cancer proliferation, invasion, and metastasis. To screen stroma-associated proteins involved in nasopharyngeal carcinoma (NPC) carcinogenesis, laser capture microdissection (LCM) and quantitative proteomic analysis were employed to assess different protein expression of the stroma between NPC and normal nasopharyngeal mucosa (NNM). In this study, periostin was identified to be significantly up-regulated in NPC stroma compared with NNM stroma and the result was further confirmed by Western blotting. Immunohistochemistry showed that over-expression of periostin was frequently observed in the stroma of NPC and matched lymph node metastases (LNM) compared with the stroma of NNM. Statistical analysis showed over-expression of periostin was significantly associated with advanced clinical stage ($P < 0.001$) and lymph node metastasis ($P < 0.001$) and decreased overall survival ($P < 0.001$) in NPC. Cox regression analysis indicated over-expression of periostin was an independent prognostic factor. Furthermore, ectopic expression of periostin was used to examine its effect on invasiveness of NPC cell in vitro and the result showed that periostin was able to promote invasiveness of NPC cell. In conclusion, periostin expression is correlated with tumor stage, lymph node metastasis, and patient survival. Periostin is a potential biomarker for the differentiation and prognosis of NPC, and it might play an important role in the progression of NPC.

Keywords Nasopharyngeal carcinoma · Periostin · Stroma · 2D-DIGE · Invasion · Disease progression

M. Li · Y. Xie · J. Shi
Department of Histology and Embryology, School of Medicine, University of South China, 421001 Hengyang, China

C. Li · G. Li · M. Li · P. Zhang · F. Peng · Z. Xiao · Z. Chen (✉)
Key Laboratory of Cancer Proteomics of Chinese Ministry of Health, Xiangya Hospital, Central South University, 87# Xiangya Road, 410008 Changsha, Hunan, China
e-mail: chenzhuchu@126.com

D. Li
Department of Oncology, Nanfang Hospital, Southern Medical University, 510515 Guangzhou, China

G. Li
School of Life Science and Technology, University of South China, 421001 Hengyang, China

Y. Guan
Cancer Research Institute, Xiangya School of Medicine, Central South University, 410078 Changsha, China

Abbreviations

NPC	Nasopharyngeal carcinoma
NNM	Normal nasopharyngeal mucosa
LCM	Laser capture microdissection
LNM	Lymph node metastases
TS	Tumor stroma
NS	Normal stroma
2D-DIGE	Two-dimensional difference gel electrophoresis
MS	Mass spectrometry

Introduction

Over the past decade, tumor microenvironment has increasingly been recognized to play a critical role in cancer development and progression [1–5]. Stromal cell-

epithelial cell interactions play an important role in tumor proliferation, invasion and metastasis [4, 6, 7]. The stromal cell involved in the constitution of tumor mass is the source of many signals which drive the proliferation and invasion of cancer cells [8] and the phenotype of tumor are largely determined by the interaction between cancer cells and their microenvironment. So analysis of the cancerous stroma is of pivotal importance to better understand cancer.

Nasopharyngeal carcinoma (NPC) is a high-incidence malignancy in southern China and Southeast Asia, and it poses a major public health problem in southern China [9]. The etiological factor is believed to be the interaction between genetic susceptibility and environmental factors, especially EBV [10, 11]. The 5-year survival rate for patients with NPC remains 50–60 %, and the majority of patients succumb to invasion and metastasis [12, 13]. To reveal the molecular mechanisms of NPC carcinogenesis, numerous efforts have been made at genes and proteins level [14], and a variety of factors are found to be involved in this highly sophisticated process [14–18], however, the carcinogenic mechanism remains poorly understood.

Investigating tumor-associated genes or proteins is crucial in understanding the molecular basis of tumor and in developing new biomarkers which can serve as methods of early detection as well as targets for novel treatment. To gain a more profound insight into NPC biology, molecular techniques and proteomic techniques have been performed to identify the tumor-specific protein [14, 19, 20]. However, very few of these signatures were confirmed in the bulk of clinical specimens and none of these markers has been widely used in the clinic, and yet there have been no reports of proteomic research on the stroma of NPC.

Two-dimensional difference gel electrophoresis (2D-DIGE) is a quantitative proteomics method with great sensitivity and accuracy of quantitation. Using the 2D-DIGE approach, different samples prelabelled with mass- and charge- matched fluorescent cyanine dyes are co-separated in the same 2D gel, and an internal standard is used in every gel, overcoming the problem of inter-gel variation. Therefore, 2D-DIGE is able to efficiently provide accurate and reproducible differential expression values for proteins in two or more biological samples [21, 22]. Using clinical tissue samples may be the most direct and persuasive way to find differential expression proteins from tumor stroma (TS) and normal stroma (NS) by a proteomic approach. However, a major obstacle in analyzing tumor specimens is tissue heterogeneity. Laser capture microdissection (LCM) has been well established as a tool for purifying cells from tissues, overcoming the problem of tissue heterogeneity and cell contamination.

To discover stroma associated proteins of NPC, LCM was used to isolate stroma cells from NPC and NNM tissue, 2D-DIGE and mass spectrometry (MS) were applied to identify differential expression proteins. Among the identified twenty differential expression proteins, periostin was an interesting protein showing up-regulation in NPC stroma and was further studied. The expression of periostin was verified by Western blotting. The secretory protein periostin, a mesenchyme-specific gene, is normally expressed in osteoblasts. It has a typical signal peptide sequence at its N terminus and four repeated domains and each of the latter shares a structural homology to insect fasciclin I [23]. The human periostin is located in chromosome 13q [24], which encodes a protein of 811 amino acids with a molecular weight of 90.2 kDa [25]. Gillan et al. [26] have found that periostin promotes adhesion and potentiates cancer cell motility through binding to integrins $\alpha v\beta 3$ and $\alpha v\beta 5$. More importantly, clinical studies of periostin expression in human cancers have demonstrated that increased expression of periostin is correlated with apoptosis, cell transformation, cell growth, cell survival, epithelial-mesenchymal transition (EMT), tumor angiogenesis and metastasis [26–37]. However, there have been very few reports on the association of periostin with NPC, and the biological functions of periostin and its significance in NPC are still unknown. Thus, we further evaluated the association between periostin expression and clinicopathological factors by immunohistochemistry, and determined its prognostic significance by analyzing the correlation between periostin expression and survival. Based on these studies, we found that periostin has a critical role in NPC progression.

Materials and methods

Materials and regents

Protease inhibitor cocktail tablets were purchased from Roche Molecular Biochemicals (Indianapolis, IN, USA). Immobiline pH-gradient (IPG) DryStrips (pH 4–7 NL, 24 cm), IPG buffer (pH 4–7), DryStrip cover fluids, thiourea, urea, DTT, Pharmalyte (pH 4–7), bromophenol blue, silver stain, molecular weight marker were purchased from Amersham Biosciences (Stockholm, Sweden). Trisbase, Bis, acrylamide, TEMED, CHAPS, SDS, glycine, acetonitrile, second antibodies-conjugated with horseradish peroxidase, mercaptoethanol, iodoacetamide, methanol, crystal violet, the enhanced chemiluminescence (ECL) system a-cyano-4-hydroxycinnamic acid (CCA), methyl green, dimethylformamide (DMF) and HCl were obtained from Sigma–Aldrich (St. Louis, MO, USA). Trypsin (sequencing grade), RPMI 1640 medium was purchased from Promega (Madison, WI, USA). PVDF membrane was obtained from Millipore (Boston, MA, USA). pCMV-neo-periostin plasmid and pCMV-neo-vector were gifted by

professor Rong Shao (University of Massachusetts, USA) kindly. Rabbit polyclonal antibody against periostin was from Abcam Inc. (Cambridge, MA, USA). Lipofectamine 2000, RPMI 1640 medium and fetal bovine serum (FBS) were obtained from Invitrogen (Invitrogen, Carlsbad, CA). 24-well transwell chambers were from Costar (Costar, Cambridge, MA, USA). Collagen matrix was purchased from Matrigel (Matrigel, Collaborative Biomedical Products, Bedford, MA, USA). TFA was purchased from Merck (Schuchardt, Hohenbrunn, Germany). All buffers were prepared using Milli-Q deionized water.

Patients and cell culture

For 2D-DIGE and Western blotting, 42 cases of fresh NPC tissue and 42 cases of fresh NNM tissue were obtained from Xiangya Hospital of Central South University, China. All samples were confirmed by histopathology before LCM. All the patients and healthy individuals signed an informed consent form for the study which was reviewed by the Institutional Review Board. The study was approved by the ethnics committee of Xiangya School of Medicine, Central South University, China. For immunohistochemical analysis, the paraffin-embedded 132 primary NPC specimens (92 males and 40 females, age 31–78 (average 55 ± 7) years, TNM staging II–IV), 30 cases of NNM, 20 cases of cervical lymph-node metastatic NPC (LMNPC) were obtained from the Department of Pathology, Xiangya Hospital. All the patients recruited in this study received neither chemotherapy nor radiotherapy before diagnosis. All specimens were handled and made anonymous according to the ethical and legal standards. For in vitro assay, the four established human NPC cell lines (6-10B, 5-8F, CNE1, and CNE2) and NIH/3T3 cell line were cultured in RPMI 1640 medium, supplemented with 10 % fetal bovine serum (FBS) and incubated at 37°C with 5 % CO. The four established human NPC cell lines (6-10B, 5-8F, CNE1, and CNE2) and NIH/3T3 cell line were used for Western blotting and in vitro assay. 6-10B without metastatic potential and 5-8F with high metastatic potential were kindly provided by Dr. H. M. Wang of the Cancer Center, Sun Yat-sen University, China [38]. Well-differentiated CNE1 and poorly differentiated CNE2 are established NPC cell lines [39]. NIH/3T3 cell line was obtained from ATCC. Cells were cultured in RPMI-1640 medium (Invitrogen, Carlsbad, CA) supplemented with 10 % fetal bovine serum (FBS) incubated at 37°C with 5 % CO_2.

LCM

Laser capture microdissection (LCM) was performed using a Leica AS LMD system (Leica) as described previously [14]. Frozen sections (8 μm) from NPC or NNM were prepared using a Leica CM 1900 cryostat (Leica) at −25°C. The sections were placed on membrane-coated glass slides (Leica), fixed in 75 % alcohol for 30 s and stained with 0.5 % violet-free methyl green (Sigma). The stained sections were air-dried and then subjected to LCM. Each cell population was determined to be 95 % homogeneous by microscopic visualization of the captured cells. Every ten cases of thirty microdissected tumor stroma (TS) or normal stroma (NS) were pooled into a set to obtain triplicate biological replicates.

Sample preparation and protein labeling

After bleaching with 70 % chilled alcohol, the microdissected cells were dissolved in lysis buffer [30 mM Tris, 7 M urea, 2 M thiourea, 4 % w/v 3-[(3-Cholamidopropyl) dimethylammonio] propanesulfonic acid (CHAPS), pH 8.5] on ice for 1 h with intermittent sonication, and then centrifuged at 12,000 rpm for 30 min at 4°C. The supernatant was collected and adjusted to pH 8.5. The concentration of the total proteins was determined using a 2-D Quantification Kit (Amersham Biosciences). Samples were labeled with *N*-hydroxy succinimidyl ester-derivatives of the cyanine dyes Cy2, Cy3, and Cy5 (Amersham Biosciences, Inc.) following a standard protocol. Equal amount proteins from all six sets of samples were pooled together as the internal standard. Three TS sets and three NS sets were randomly labeled with Cy3 or Cy5, while internal standards were labeled with Cy2, using 400 pmol fluorochrome/50 μg protein. Labeling reactions were performed on ice in the dark for 30 min and then quenched by the addition of 1 μl 10 mM lysine (Sigma) for 10 min.

2D-DIGE and gel imaging

Cy3- and Cy5- labelled samples (50 μg) from each set of the TS and NS groups were mixed and run on the same gels before mixing with 50 μg Cy2-labelled internal standards. An equal volume of 2× sample buffer [(8 M urea, 2 M thiourea, 4 % CHAPS, 2 % Bio-lyte, pH 4–7, 130 mM dithiothreitol (DTT)] was added to the sample and the total volume was filled up to 450 μl with rehydration buffer (8 M urea, 4 % CHAPS, 1 % Biolyte, pH 4–7, 13 mM DTT). The proteins were applied to IPG strips [pH 4–7; nonlinear (NL), 24 cm) and focused on an IPGphor (Amersham Biosciences). The focused IPG strips were equilibrated and then transferred onto 12 % SDS polyacrylamide gels (SDS-PAGE) poured between low fluorescence glass plates on an Ettan DALT II system (Amersham Biosciences). All electrophoresis procedures were performed in the dark. The biological triplicate TS and NS sets and the internal standard were run on three gels as analytic gels. After SDS-PAGE, the three analytic gels

were collected on a Typhoon 9410 scanner (GE Healthcare) to generate nine protein spot maps. After scanned, the DIGE gels were post-stained with silver stain. Statistics and quantitation of protein expression were carried out in Decyder 5.0 software (GE Healthcare) according to the manufacturer's recommendations. The differential expression protein spots ($|ratio|_{TS/NS} \geq 1.5$, $P \leq 0.05$) that altered consistently in all nine protein-spot maps were selected for identification.

Protein identification by mass spectrometry

Differential expression protein spots of interest were excised from the preparative gel, destained, and in-gel trypsin digested as described previously [14]. Tryptic peptides (0.5 μl) were mixed with 0.5 μl matrix [4-hydroxy-α-cyanocinnamic acid (HCCA) in 30 % ACN/0.1 % TFA] and then analysed using a Voyager System DESTR 4307 MALDI-TOF mass spectrometer (ABI) to obtain the peptide mass fingerprint (PMF). Peptide matching and protein searches against the NCBInr database were performed using the Mascot search engine (http://www.matrixscience.com/) with a mass tolerance of ±50 ppm. The protein spots not identified by MALDI-TOF were also subjected to analysis of ESI-Q-TOF-MS (Micromass). MS/MS spectra were collected in data-dependent mode in which up to four precursor ions above an intensity threshold of seven counts/s were selected for MS/MS analysis from each survey "scan". In tandem mass spectrometry data database query, the peptide sequence tag (PKL) format files that were generated from MS/MS were imported into the Mascot search engine with a MS/MS tolerance of ±0.3 Da to search the NCBInr database according to parameters as follows: the fixed modifications were selected as carbamidomethyl (cysteine); the variable modification was selected as oxidation (methionine).

Western blotting

Proteins isolated from 12 pairs of microdissected stroma of fresh NPC and NNM, four NPC cell lines (6-10B, 5-8F, CNE1, CNE2), and NIH/3T3 cell line were used for Western blotting. Briefly, 40 μg of lysates were separated by 10 % SDS polyacrylamide gels and transferred to PVDF membrane (Bio-Rad). The blots were incubated with anti-periostin (1:3,000 dilution; Abcam) and then incubated with a horseradish peroxidase-conjugated secondary antibody. Immunoreactive bands were detected by using chemiluminescence and quantitated by densitometry using ImageQuant image analysis system (Storm Optical Scanner). The mouse anti-β-actin (1:5,000 dilution; Sigma) was detected simultaneously as a loading control.

Fig. 1 Representative 2D-DIGE maps of the stroma of NNM and NPC tissues and MALDI-TOF–MS analysis of the differential expression protein periostin. **a** Protein lysates of the internal standard were labeled with Cy2. **b** Protein lysates of microdissected NNM stroma were labeled with Cy3 (*green,* NS). **c** Protein lysates of microdissected NPC stroma were labeled with Cy5 (*red,* TS). **d** Representative 2D-DIGE gel which was post-stained with silver staining, and the differential expression proteins were marked with arrows. **e** *left*, zoomed image of differential expression protein spot 10; *right*, three-dimensional simulation of protein spot 10. **f** MALDI-TOF–MS analysis of differential expression protein spot 10; *top,* the MALDI-TOF–MS mass spectrum of spot 10 was identified as periostin according to the matched peaks; *bottom*, protein sequence of periostin was shown, and matched peptides are labeled in *red letters*. (Color figure online)

Cell transfection

pCMV-neo-periostin plasmids (gift of professor Rong Shao, University of Massachusetts, USA) and empty vector pCMV-neo were transfected into 6-10B cells with the Lipofectamine 2000 Reagent (Invitrogen) according to the transfection protocol provided by the manufacturer. At the end of the transfection, the expression level of periostin was determined by Western blotting.

In vitro cell invasion assay

Cell invasion assays were performed over 48 h using Matrigel-coated 8 μm pore size trans-well chambers (Costar, Cambridge, MA) using 6-10B cells transfected with periostin plasmid or empty vector [40]. After cells (1.5×10^6 cells/ml) were placed in the upper compartment, the lower chambers of the trans-well were filled with 500 μl of medium with 10 % FBS as a chemo-attractant. Non-invasive cells and matrigel were removed by scraping with sterile cotton swabs. Cells invading the lower chamber were stained with a Diff-Quik stain kit (Dade Behring, Newark, DE) and counted under a microscope at 200× magnification and 10 fields were randomly selected and counted for each assay. Three independent experiments were performed in triplicate.

Immunohistochemistry staining

Immunohistochemistry was done on formalin-fixed, paraffin-embedded specimens with anti-periostin (1:1,000 dilution, abcam), according to the manufacturers' protocols. A standard avidin–biotin complex technique was employed, with citrate buffer microwave antigen retrieval. Immunostaining was blindly evaluated by two independent experienced pathologists in an effort to provide a consensus on staining patterns according to a scoring method as described by Daniel Marsh [5]. Staining for periostin was scored, at least 10 high-power fields, selected randomly, according to the extent of stromal positivity, as low/

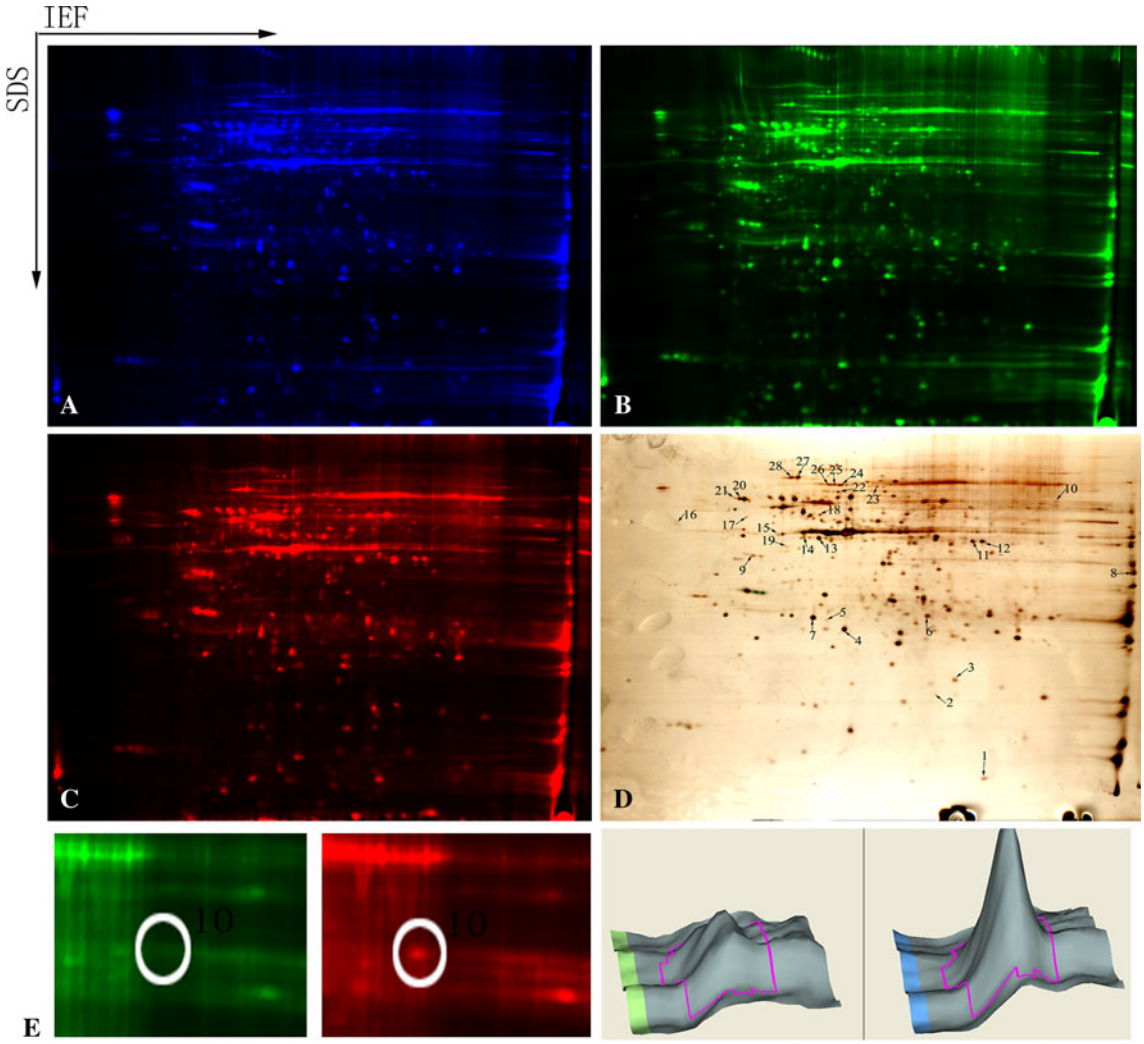

F

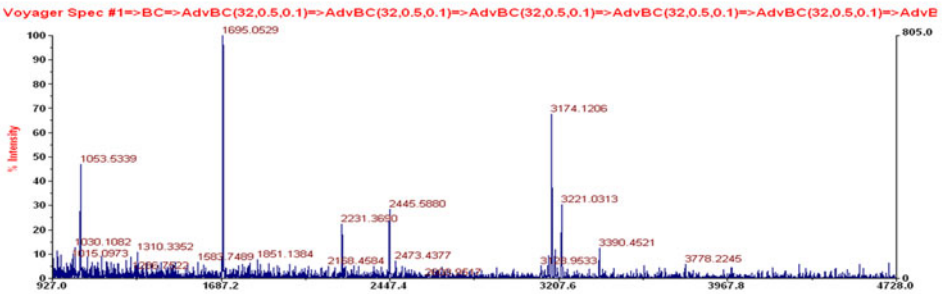


```
  1 MIPFLPMFSL LLLLIVNPIN ANNHYDKILA HSRIRGRDQG PNVCALQQIL
 51 GTKKKYFSTC KNWYKKSICG QKTTVLYECC PGYMRMEGMK GCPAVLPIDH
101 VYGTLGIVGA TTTQRYSDAS KLREEIEGKG SFTYFAPSNE AWDNLDSDIR
151 RGLESHVNVE LLNALHSHMI NKRMLTKDLK NGMIIPSMYN NLGLFINHYP
201 NGVVTVNCAR IIHGNQIATN GVVHVIDRVL TQIGTSIQDF IEAEDDLSSF
251 RAAAITSDIL EALGRDGHFT LFAPTNEAFE KLPRGVLERI MGDKVASEAL
301 MKYHILNTLQ CSESIMGGAV FETLEGNTIE IGCDGDSITV NGIKMVNKKD
351 IVTNNGVIHL IDQVLIPDSA KQVIELAGKQ QTTFTDLVAQ LGLASALRPD
401 GEYTLLAPVN NAFSDDTLSM DQRLLKLILQ NHILKVKVGL NELYNGQILE
451 TIGGKQLRVF VYRTAVCIEN SCMEKGSKQG RNGAIHIFRE IIKPAEKSLH
501 EKLKQDKRFS TFLSLLEAAD LKELLTQPGD WTLFVPTNDA FKGMTSEEKE
551 ILIRDKNALQ NIILYHLTPG VFIGKGFEPG VTNILKTTQG SKIFLKEVND
601 TLLVNELKSK ESDIMTTNGV IHVVDKLLYP ADTPVGNDQL LEILNKLIKY
651 IQIKFVRGST FKEIPVTVYT TKIITKVVEP KIKVIEGSLQ PIIKTEGPTL
701 TKVKIEGEPE FRLIKEGETI TEVIHGEPII KKYTKIIDGV PVEITEKETR
751 EERIITGPEI KYTRISTGGG ETEETLKKLL QEDTPVRKLQ ANKKVQGSRR
801 RLREGRSQ
```

negative (<5 % stroma positive), moderate (patchy/focal expression, 5–50 % stroma positive) or high (diffuse expression throughout tumor, >50 % stroma positive). Concordance was greater than 95 %, confirming the objectivity of the scoring method. Remaining cases were re-analyzed and a consensus score was agreed.

Statistical analysis

All statistical analyses were performed with SPSS 14.0 software. One-way ANOVA, the Mann–Whitney *U*-test or the Kruskal–Wallis test were used to evaluate the relationships between periostin expression and clinicopathological factors. Follow-up for NPC patients by telephone was carried out to obtain the information of patients' outcomes. The follow-up period lasted up to 60 months. At the time of last follow-up, the data were censored if patients still alive or lost to follow-up. Overall survival was calculated from time of surgery to time of death from any cause. Survival rates (Cumulative survival, Cumulative survival curves) were obtained by the Kaplan–Meier method, and log-rank testing was used to evaluate the statistical significance of difference. The deaths caused by NPC were considered as outcomes; the deaths by other causes were censored and the missing values were replaced by the series mean method. Cox regression analysis was used to evaluate the prognostic significance of clinicopathological factors. For all analyses, $P < 0.05$ was considered to be statistically significant.

Results

Identification of differential expression proteins by 2D-DIGE and MS

Proteins extracted from the stroma of NPC and NNM were separated by 2-DIGE. The representative 2-DIGE maps were shown in Fig. 1a–c, proteins of the internal standard, NNM and NPC were labeled with fluorescent dyes Cy2, Cy3 and Cy5 respectively. The interchangeable use of either Cy3 or Cy5 for either pooled set has already been built. After 2D-DIGE, the Cy2, Cy3 and Cy5 images were scanned, and analyzed using DeCyder 5.0 software to detect the differentially expressed proteins between NPC and NNM. And all DIGE gels were post-stained with silver staining to excise the differential expression protein spots visually. After comparing the average abundance changes, a total of 28 differential expression protein spots (≥1.5-fold variation) in the two types of tissues were detected, and 20 differential expression proteins were identified successfully by the analysis of both MALDI-TOF-MS and ESI-Q-TOF MS. The 28 differential expression protein spots were marked with arrows in Fig. 1d and their information identified by MS was listed in Table 1. Among them, protein spot 10 was significantly up-regulated in NPC stroma compared to NNM stroma (Average ratio = 2.38, $P = 0.0013$), and its close-up of the region of 2D-DIGE gel images and three-dimensional simulation were showed in Fig. 1e. MALDI-TOF-MS analysis and database matching identified spot 10 as periostin with high sequence coverage and mass accuracy (Fig. 1f).

Validation of periostin expression by Western blotting

Western blotting was done to validate differential expression of periostin in 12 pairs of microdissected stroma of NPC and NNM. As shown in Fig. 2a, periostin was significantly up-regulated in the stroma of NPC compared with NNM ($P = 0.002$), which confirms the result of 2D-DIGE analysis.

Expression of periostin in NPC cell lines and NIH/3T3 cell line

Western blotting was also done to detect the expression of periostin in four NPC cell lines (CNE1, CNE2, 6-10B, 5-8F) and NIH/3T3 cell line. As shown in Fig. 2b, periostin was not present in CNE1, CNE2, 6-10B and NIH/3T3 cell lines, while was slightly expressed in 5-8F cells with high metastatic potential. The results indicated that periostin was a stromal protein, and was related to metastatic potential of NPC cell lines.

Over-expression of periostin promotes cell invasion in vitro

To study the association of periostin up-regulation in 6-10B cell line with its invasive ability, 6-10B cells, which had no expression of periostin and without metastatic potential were transfected with pCMV-neo-periostin plasmid, and the expression of periostin was determined by Western blotting. As shown in Fig. 3a, introduction of pCMV-neo-periostin plasmids into 6-10B cells significantly increased periostin expression compared with control 6-10B cells. We then performed cell invasion assays to evaluate the effect of up-regulation of periostin in 6-10B cells. As shown in Fig. 3b and c, 6-10B cells transfected with pCMV-neo-periostin plasmids showed an absolutely increased invasive ability than control 6-10B cells ($P < 0.05$). These results showed the direct functional role of periostin in promoting tumor cell invasion.

Expression of periostin in NNM and primary and metastatic NPC

To determine the distribution and clinical significance of periostin in NNM and Primary and Metastatic NPC, we

Table 1 The differential proteins between TS and NS identified by MS

No	Protein name	Protein AC	Mass	pI	Sequence coverage (%)	Protein function	Av. ratio*
1	Mrp14 (migration inhibitory factor-related protein 14) (S100A9)	gil20150229	13,159	5.71	76	Signal transduction and cell communication	2.42
2	Superoxide dismutase [Cu–Zn]	gil31615344	16,154	5.7	68	Energy pathways	−1.89
3	Nm23 protein	gil35068	20,746	7.07	25	Signal transduction and cell communication	1.99
4	Chain A, crystal structure of lipid-free human apolipoprotein A-I	gil90108664	28,061	5.27	26	Transport	−1.63
5	Proapolipoprotein	gil178775	28,944	5.45	54	Transport	1.67
6	PYCARD protein	gil48257192	21,326	5.67	43	Apoptosis	1.93
7	Rho GDP dissociation inhibitor (GDI) beta	gil56676393	23,031	5.10	77	Signal transduction and cell communication	−2.61
8	Heterogeneous nuclear ribonucleoprotein A2/B1	gil73976124	32,524	8.74	24	Signal transduction and cell communication	−1.61
9	Nucleolar phosphoprotein B23	gil190238	9,246	9.72	17	Signal transduction and cell communication	−1.52
10	Periostin, osteoblast specific factor	gil5453834	93,901	7.57	63	Signal transduction and cell communication	2.38
11	Gelsolin-like capping protein isoform 9	gil55597035	38,779	5.88	52	Cell growth and/or maintenance	2.67
12	Gelsolin-like capping protein isoform 9	gil55597035	38,779	5.88	27	Cell growth and/or maintenance	2.67
13	Cytokeratin-19	gil90111766	44,065	5.04	21	Cell growth and/or maintenance	−1.61
14	Cytokeratin-1	gil1346343	66,149	8.16	25	Cell growth and/or maintenance	1.55
15	Ribosomal protein SA, isoform CRA_c	gil119584991	19,853	8.37	55	Signal transduction and cell communication	1.66
16	Cytokeratin-1	gil1346343	66,149	8.16	25	Cell growth and/or maintenance	1.55
17	Heterogeneous nuclear ribonucleoprotein H1	gil5031753	49,484	5.89	27	Signal transduction and cell communication	−2.59
18	Protein disulfide isomerase	gil1710248	46,512	4.95	33	Protein metabolism	1.81
19	C protein	gil306875	32,004	5.10	53	Signal transduction and cell communication	−2.19
20	Prolyl 4-hydroxylase	gil20070125	57,480	4.76	34	Protein metabolism	2.03
21	Prolyl 4-hydroxylase	gil20070125	57,480	4.76	34	Protein metabolism	2.03
22	Transformation upregulated nuclear protein	gil460789	51,325	5.13	54	Signal transduction and cell communication	−1.52
23	L-plastin variant	gil62898171	70,785	5.2	58	Cell growth and/or maintenance	−2.02
24	Heat shock 70 kDa protein 8 isoform 1	gil5729877	71,082	5.37	29	Protein metabolism	−1.56
25	L-plastin isoform 3	gil114651523	70,815	5.2	63	Protein metabolism	−2.34
26	L-plastin isoform 3	gil114651523	70,815	5.2	59	Cell growth and/or maintenance	−1.56
	Heat shock 70 kDa protein 8 isoform 1	gil5729877	71,082	5.37	29	Protein metabolism	−1.56
27	GRP78 precursor	gil386758	72,185	5.03	71	Protein metabolism	1.59
28	BiP protein	gil6470150	71,002	5.23	68	Protein metabolism	1.71

* Av. Ratio, TS group/NS group

analyzed the expression pattern of periostin by using immunohistochemistry in archival clinical tissues including 132 cases of primary NPC, 30 cases of NNM, and 20 cases of cervical LMNPC. As shown in Fig. 4, in NNM, periostin was slightly expressed in capillary endothelial cells, fibroblasts, basilar membrane (Fig. 4a). In NPC and LMNPC tissue, strong periostin expression was observed close to the neoplastic cells in the neoplastic stroma, while no periostin

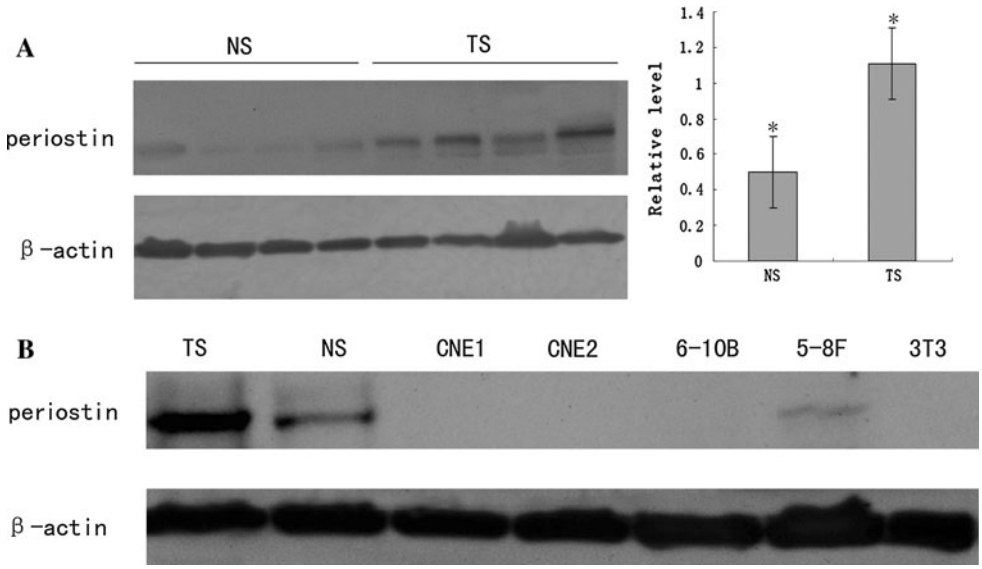

Fig. 2 Representative Western blotting results of periostin expression in microdissected stroma and cell samples. **a** *left* Western blotting shows different expression levels of periostin between TS and NS; *right* Histogram shows the relative expression levels of periostin in 12 cases of NS and 12 cases of TS as determined by densitometric analysis ($P = 0.002$). **b** Western blotting shows changes in the expression level of periostin in NPC cell lines (6-10B, 5-8F, CNE2, CNE1) and NIH/3T3 cell line. β-actin is used as the internal loading control

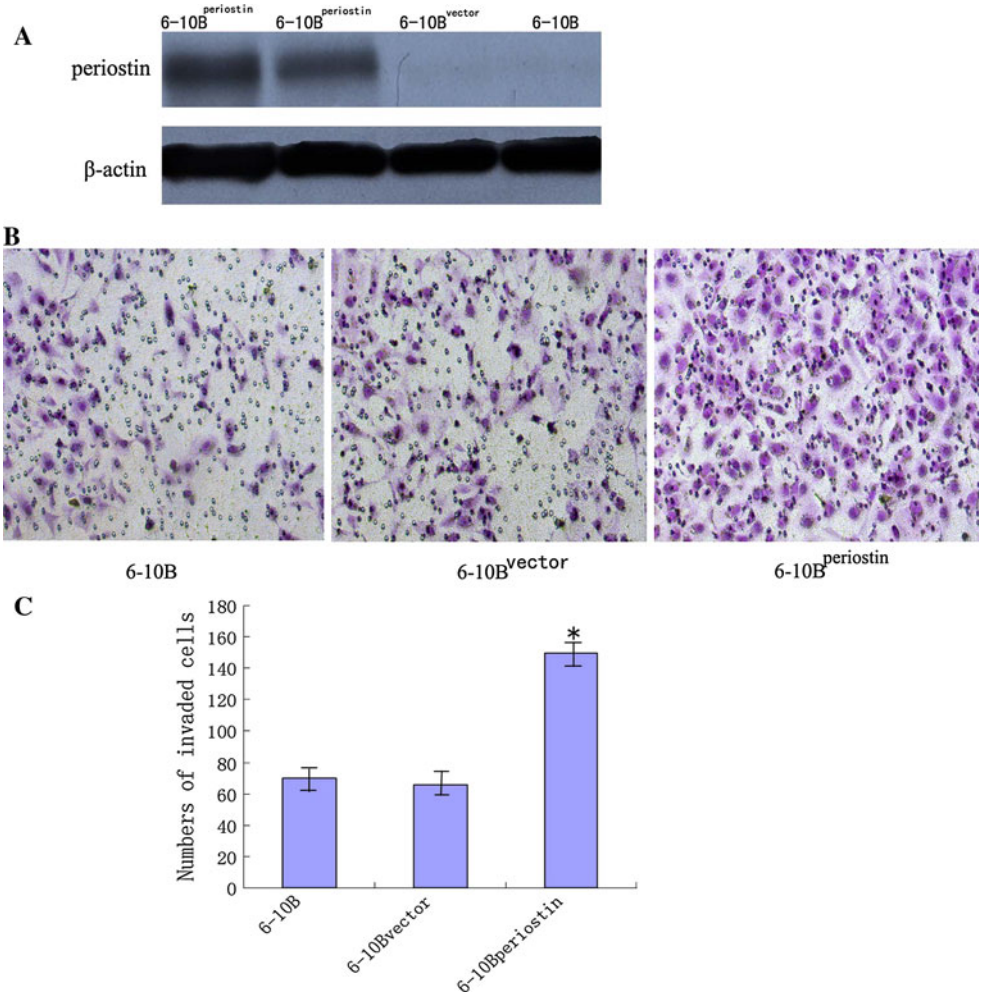

Fig. 3 In vitro cell invasion assay of pCMV-neo-periostin plasmid transfected (6-10B^{periostin}) and control 6-10B cells (6-10B^{vector}, 6-10B). **a** Western blotting showing the expression level of periostin in 6-10B^{periostin} and control 6-10B cells. **b** The invasion of 6-10B^{periostin} and control 6-10B cells was measured by using transwell chambers. Tumor cells penetrating the precoated polycarbonate membrane were photographed. **c** The numbers of invasive tumor cells per field in 6-10B^{periostin} and control 6-10B cells ($P < 0.05$)

expression was observed in cancer cells and inflammatory cells (Fig. 4b, c, d). And compared with NNM, stronger staining of periostin was observed in primary NPC and lymph node metastasis. Statistical analysis indicated that periostin expression was significantly up-regulated in primary NPC versus NNM, and periostin expression in

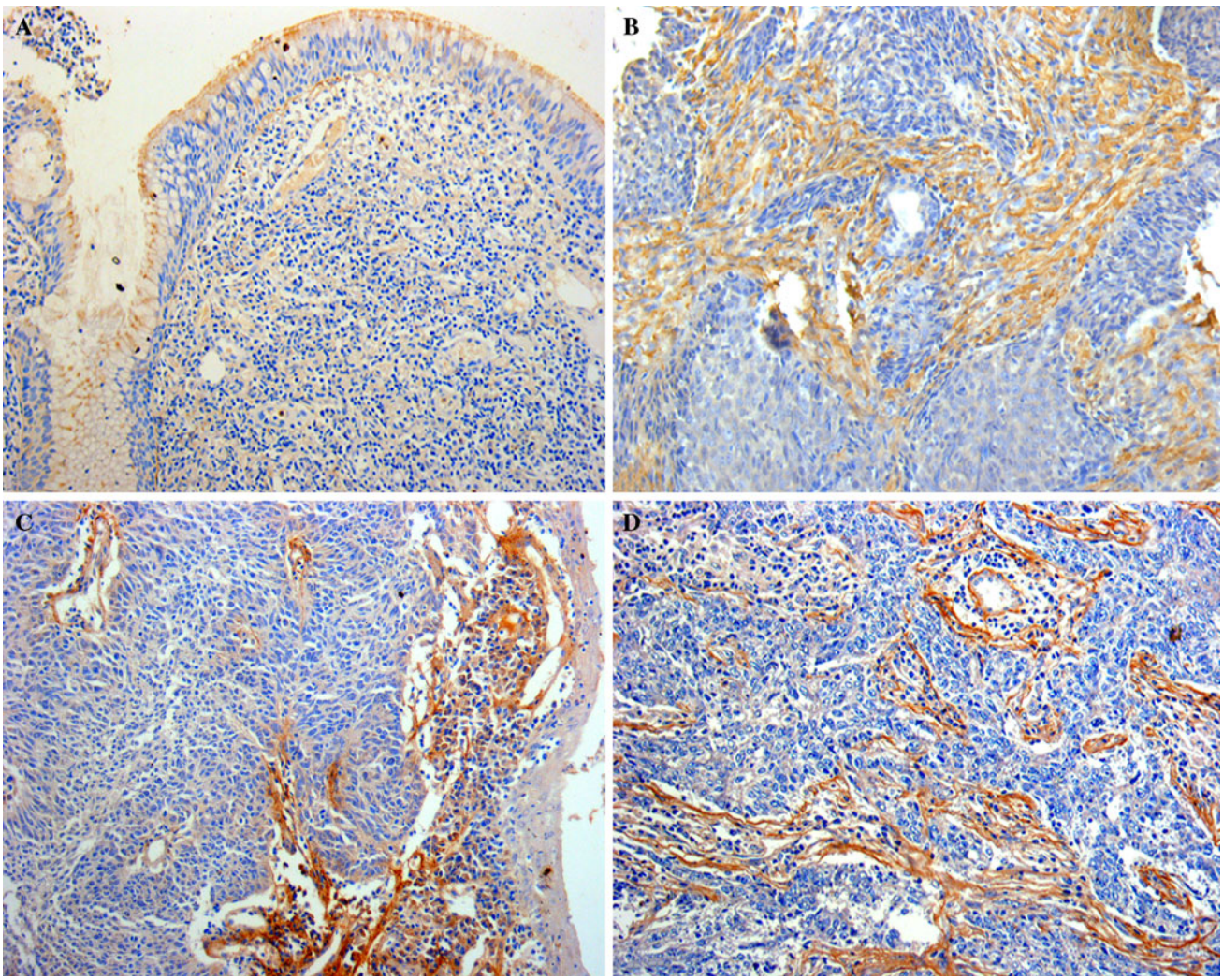

Fig. 4 Representative photographs of immunohistochemistry of periostin expression in the tissue specimens. **a** Weak staining in the stroma of NNM; **b** moderate staining in the stroma of primary NPC (WHOII); **c** strong staining in the stroma of primary NPC (WHOIII); **d** strong staining in the stroma of positive LMNPC. No staining was detectable in the nasopharyngeal epithelial cells, inflammatory cells and cancer cells. Original magnification: ×200

LMNPC was higher than the primary NPC (Table 2). The results indicated that dysregulation of periostin might be related to development and metastasis of NPC.

Correlation of Periostin expression in primary NPC with clinicopathological factors

The relationships between clinicopathological factors and periostin expression are shown in Table 3. Periostin expression levels were correlated with histologic type/grade, clinical stage, recurrence, and regional lymph node and distant metastasis (Table 3). Type III (poorly differentiated) NPC showed a more intense immunoreactivity of periostin compared with type II (moderately differentiated) NPC (Fig. 4; Table 3). An increase in periostin expression in NPC was found to be significantly associated with advanced clinical stage, more frequent recurrence, and lymph node metastasis. No significant correlations were found between periostin expression and other characteristics, including gender, age and the primary tumor (T) stage.

To undermine the prognostic significance of periostin in NPC, the association of expression level of periostin with patients' survival was further evaluated. Survival curves were calculated for a total of 132 cases of NPC patients. By the end of the study, 63 of 132 patients had died, 67 patients were still alive, and two patients were lost to follow-up, 2 patients had died of unrelated causes. The mean survival rate was 54.99 ± 1.16 months in the low- and moderate- periostin protein expression group ($n = 98$), but it was only 29.82 ± 3.35 months in the high periostin protein expression group ($n = 34$). The survival curves showed that the overall survival rate was significantly

Table 2 The difference of periostin expression among NNM, NPC and LMNPC

Tissues	*n*	Score			*P*
		Low	Moderate	High	
NNM	30	18	9	3	0.000[a]
NPC	132	22	76	34	0.010[b]
LMNPC	20	2	5	13	

[a] $P < 0.01$ by Mann–Whitney U test, NNM versus NPC

[b] $P < 0.01$ by Mann–Whitney U test, NPC versus LMNPC

Table 3 Associations of periostin expression with clinicopathological factors in NPC

Variables	*n*	Score			*P*
		Low	Moderate	High	
Gender					
Male	92	20	50	22	0.705
Female	40	2	26	12	
Age (years)					
≥50	62	10	36	16	0.472
<50	70	12	40	18	
WHO type					
Type II	30	12	16	2	0.016*
Type III	102	10	60	32	
Primary tumor(T) stage					
T1	36	4	22	10	0.464
T2	46	10	24	12	
T3	40	6	26	8	
T4	10	2	4	4	
Regional lymph node(N) metastasis					
N0	17	12	5	0	0.000*
N1	21	5	10	6	
N2	61	3	46	12	
N3	33	2	15	16	
Distant metastasis (M)					
M0	112	22	66	24	0.000*
M1	20	0	10	10	
Clinical stage					
II	14	8	4	2	0.000*
III	76	12	48	16	
IV	42	2	24	16	
Recurrence					
Negative	92	20	64	8	0.000*
Positive	40	2	12	26	

* $P < 0.05$ or 0.01 by Mann–Whitney test or Kruskal–Wallis H test

decreased with increasing periostin expression (Fig. 5). In univariate analysis (Table 4), decreased survival was correlated with histologic type, regional lymph node metastasis, distant metastasis, recurrence, and increasing periostin expression ($P < 0.05$). In multivariate analysis

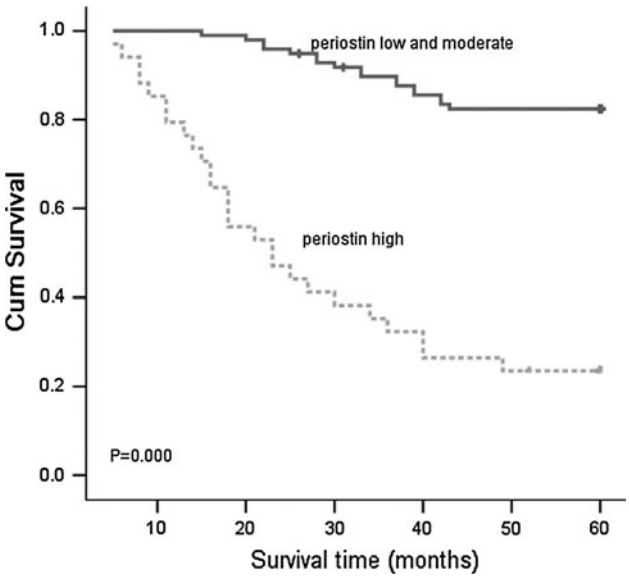

Fig. 5 Kaplan–Meier survival plots for NPC patients according to the expression levels of periostin. Kaplan–Meier survival analysis showed that the cumulative 5-year survival rate was 54.99 ± 1.16 months in the low- and moderate- periostin protein expression group ($n = 98$), but it was only 29.82 ± 3.35 months in the high expression group ($n = 34$). P was determined by a two-sided log-rank test

(Table 5), only regional lymph node metastasis, distant metastasis, recurrence, and increased periostin expression remained as the significant independent prognostic factors of decreased overall survival rate ($P < 0.05$).

Discussion

In this study, we combined proteomic method with LCM to directly investigate the differential expression protein profiles between the stroma of NPC and NNM. 20 differential expression proteins were successfully identified, which are involved in a variety of biological processes. It

Table 4 Prognostic factors by univariate analysis (Cox's proportional hazards model)

Variables	Hazard ratio (95 % confidence interval)	*P*
Age (≥50/<50)	1.00 (0.97–1.02)	0.67
Gender (male/female)	1.08 (0.63–1.86)	0.78
WHO type (II/III)	5.56 (2.23–13.87)	<0.01
Regional lymph node metastasis(N/P)	13.80 (1.91–99.54)	<0.01
Distant Metastasis (N/P)	6.09 (3.48–10.65)	<0.01
Clinical stage(II/III + IV)	2.90 (0.91–9.25)	0.07
Recurrence (N/P)	7.58 (4.51–12.72)	<0.01
Periostin (low/medium/high)	3.31 (2.19–5.02)	<0.01

N negative, *P* positive

Table 5 Significant prognostic factors by multivariate analysis (cox's proportional hazards model)

Variables	Hazard ratio (95 % confidence interval)	*P*
WHO type (II/III)	2.17 (0.82–5.72)	0.12
Regional lymph node (N) metastasis	7.98 (1.02–62.42)	<0.05
Distant metastasis (N/P)	2.40 (1.29–4.46)	<0.01
Recurrence (N/P)	4.69 (2.41–9.12)	<0.01
Periostin (low/medium/high)	1.65 (1.01–2.69)	<0.05

N negative, *P* positive

has been reported that the several up-regulated proteins in NPC such as S100A9, CapG and Nm23 played important roles in NPC progression. The over-expression of S100A9 in various types of human malignancies has been demonstrated, such as lung, prostate cancer and NPC, and it was related to cancer invasion and metastasis, and poor tumor differentiation [41, 42]. CapG up-regulation was frequently observed in various carcinomas including NPC [43–45], and could modulate invasive properties of cells during tumorigenesis. Over-expression of Nm23, specifically its nuclear translocation, may be a powerful predictor of radiation resistance in head and neck squamous cell carcinoma (HNSCC) [46]. Nm23 involved in a signaling cross-talk network and may be potential treatment targets for NPC in the future [47]. In addition, the several differential expression proteins including Superoxide Dismutase, prolyl 4-hydroxylase, protein disulfide isomerase and BiP/GRP78 involve in protein metabolism, and another several differential expression proteins such as Rho GDI-β, L-plastin and C protein correlate with signal transduction and cell communication, suggesting these proteins in stroma might be correlated with NPC carcinogenesis or progression. Among the identified proteins, perisotin showed higher statistical significance in 2D-DIGE image analysis. These results were in accordance with our previous reports [45] and confirmed the reliability of proteomics.

The source of periostin in tumor is still under debate. Recently more and more researches indicated that periostin is a matrix specific protein, with high expression in the stromal cells surrounding the carcinoma epithelium [29, 36, 48], at the same time, some researchers suggested that periostin was detected in cancer cells [30]. In our study, we found that periostin protein was not present in NPC cells as well as NPC cell lines except for the high metastasis cell line 5-8F, and had weak expression in the stroma of NNM, while has strong expression in the stroma of NPC. These findings were in accordance with previous reports [29, 36, 48]. Building on these results and previous studies, we speculate that NPC cells mediated humoral factor(s) may stimulate cancerous stroma cells to secret periostin.

Various avenues of investigation have suggested that tumor microenvironment can produce many signals promoting the proliferation and invasion of cancer cells [1–5]. The dynamic interactions between cancer and stromal cells, as well as between cancer cells and the extracellular matrix (ECM), could promote the invasion and metastasis of cancer cells by activating a variety of genes. It is well-known that metastatic spread of tumor cells is a multi-step and complicated process. To metastasize, tumor cells need to invade through the basement membrane, detach from the primary tumor mass, enter the circulation, travel to a distant secondary site, extravasate, and expand in the new environment [49]. Each of these steps is essential and many proteins play critical roles in some of these processes. Therefore, some crucial proteins involved in metastatic process can be used as biomarkers or targets for the management of NPC. In this study, very interestingly, periostin was up-regulated in NPC stroma. Periostin, a secreted protein, has been demonstrated that it can facilitate the migration and differentiation of cells to undergo EMT, both during embryogenesis and under pathological conditions [32] and plays important roles in the progression and metastasis of various types of tumors [29–31, 34, 50]. In pancreatic cancer, periostin promotes tumor cells' migration in the matrix of the microenvironment by activating the Akt/PI3K pathway and it is correlated with EMT [32]. However, the reports on the association of periostin with NPC are very little, and the biological functions of periostin and its significance in NPC remains unknown. Therefore, we further evaluated the association of periostin expression with clinicopathological factors, and determined its prognostic significance by survival analysis.

In the present study, our results demonstrated for the first time that periostin was up-regulated in the stroma of NPC versus NNM, and up-regulated in LMNPC versus primary NPC, and primary NPC with higher periostin expression tended to have later TNM clinical stage, more frequent recurrence, and lymph node and distant metastasis, suggesting periostin was associated with the progression and metastasis of NPC. We also observed that increased periostin expression significantly increased the invasive ability of 6-10B cells in vitro, supporting that periostin behaves as a metastasis promoter in NPC. In addition, univariate analysis showed that the NPC patients with periostin up-regulation in primary NPC had poor survival, and multivariate analysis further indicated that high expression of periostin was an independent prognostic indicator for decreased overall survival in NPC ($P < 0.05$). Our studies, together with previous reports, suggest that periostin plays a crucial role in tumor metastasis.

In summary, we identified 20 differential expression proteins between the stroma of NPC and NNM using a proteomic approach coupled with LCM. We further demonstrated that the differential expression protein, periostin, is a potential biomarker for metastasis and prognosis of NPC, and plays an important role in NPC progression. These findings have potential clinical value in predicting the metastasis and prognosis of NPC, and identifying NPC patients that are at high risk of progression.

Acknowledgments This research was supported by grants from National Natural Sciences Foundation of China (Grant No. 81072199, 30973289), Scientific Research Foundation for Dr. of University of South China (2010XQD38), National Basic Research Program of China (2011CB910704), Science and Technology Research Program of Hunan Province in China (2011TT2015). We gratefully acknowledge Professor Rong Shao (University of Massachusetts, USA) for providing pCMV-neo-periostin plasmid.

Conflict of interest No conflicts of interest are declared.

References

1. Albini A (2008) Tumor microenvironment, a dangerous society leading to cancer metastasis. From mechanisms to therapy and prevention. Cancer Metastasis Rev 27(1):3–4
2. Zigrino P, Loffek S, Mauch C (2005) Tumor–stroma interactions: their role in the control of tumor cell invasion. Biochimie 87(3–4):321–328
3. Sung SY et al (2007) Tumor microenvironment promotes cancer progression, metastasis, and therapeutic resistance. Curr Probl Cancer 31(2):36–100
4. Hiscox S, Barrett-Lee P, Nicholson RI (2011) Therapeutic targeting of tumor-stroma interactions. Expert Opin Ther Targets 15(5):609–621
5. Marsh D et al (2011) Stromal features are predictive of disease mortality in oral cancer patients. J Pathol 223(4):470–481
6. Wernert N et al (2001) Presence of genetic alterations in microdissected stroma of human colon and breast cancers. Anticancer Res 21(4A):2259–2264
7. Liotta LA, Kohn EC (2001) The microenvironment of the tumour–host interface. Nature 411(6835):375–379
8. Bissell MJ, Radisky D (2001) Putting tumours in context. Nat Rev Cancer 1(1):46–54
9. Yu MC, Yuan JM (2002) Epidemiology of nasopharyngeal carcinoma. Semin Cancer Biol 12(6):421–429
10. Choi PH et al (2011) Nasopharyngeal carcinoma: genetic changes, Epstein-Barr virus infection, or both. A clinical and molecular study of 36 patients. Cancer 72(10):2873–2878
11. Ali H, Al-Sarraf M (1999) Nasopharyngeal cancer. Hematol Oncol Clin North Am 13(4):837–847
12. Vokes EE, Liebowitz DN, Weichselbaum RR (1997) Nasopharyngeal carcinoma. Lancet 350(9084):1087–1091
13. Ahmad A, Stefani S (1986) Distant metastases of nasopharyngeal carcinoma: a study of 256 male patients. J Surg Oncol 33(3):194–197
14. Cheng AL et al (2008) Identification of novel nasopharyngeal carcinoma biomarkers by laser capture microdissection and proteomic analysis. Clin Cancer Res 14(2):435–445
15. Qian CN et al (2002) Met protein expression level correlates with survival in patients with late-stage nasopharyngeal carcinoma. Cancer Res 62(2):589–596
16. Hwang CF et al (2010) Fibulin-3 is associated with tumour progression and a poor prognosis in nasopharyngeal carcinomas and inhibits cell migration and invasion via suppressed AKT activity. J Pathol 222(4):367–379
17. Wang S et al (2010) TFPI-2 is a putative tumor suppressor gene frequently inactivated by promoter hypermethylation in nasopharyngeal carcinoma. BMC Cancer 10:617
18. Buettner M et al (2007) Expression of RANTES and MCP-1 in epithelial cells is regulated via LMP1 and CD40. Int J Cancer 121(12):2703–2710
19. Cho WC et al (2004) Identification of serum amyloid a protein as a potentially useful biomarker to monitor relapse of nasopharyngeal cancer by serum proteomic profiling. Clin Cancer Res 10(1 Pt 1):43–52
20. Zhou Y et al (2008) Identification of candidate molecular markers of nasopharyngeal carcinoma by microarray analysis of subtracted cDNA libraries constructed by suppression subtractive hybridization. Eur J Cancer Prev 17(6):561–571
21. Friedman DB et al (2004) Proteome analysis of human colon cancer by two-dimensional difference gel electrophoresis and mass spectrometry. Proteomics 4(3):793–811
22. Kakisaka T et al (2007) Plasma proteomics of pancreatic cancer patients by multi-dimensional liquid chromatography and two-dimensional difference gel electrophoresis (2D-DIGE): up-regulation of leucine-rich alpha-2-glycoprotein in pancreatic cancer. J Chromatogr B Analyt Technol Biomed Life Sci 852(1–2): 257–267
23. Horiuchi K et al (1999) Identification and characterization of a novel protein, periostin, with restricted expression to periosteum and periodontal ligament and increased expression by transforming growth factor beta. J Bone Miner Res 14(7):1239–1249
24. Litvin J et al (2005) Periostin family of proteins: therapeutic targets for heart disease. Anat Rec A Discov Mol Cell Evol Biol 287(2):1205–1212
25. Takeshita S et al (1993) Osteoblast-specific factor 2: cloning of a putative bone adhesion protein with homology with the insect protein fasciclin I. Biochem J 294(Pt 1):271–278
26. Gillan L et al (2002) Periostin secreted by epithelial ovarian carcinoma is a ligand for alpha(V)beta(3) and alpha(V)beta(5) integrins and promotes cell motility. Cancer Res 62(18): 5358–5364
27. Michaylira CZ et al (2010) Periostin, a cell adhesion molecule, facilitates invasion in the tumor microenvironment and annotates a novel tumor-invasive signature in esophageal cancer. Cancer Res 70(13):5281–5292
28. Ruan K, Bao S, Ouyang G (2009) The multifaceted role of periostin in tumorigenesis. Cell Mol Life Sci 66(14):2219–2230
29. Erkan M et al (2007) Periostin creates a tumor-supportive microenvironment in the pancreas by sustaining fibrogenic stellate cell activity. Gastroenterology 132(4):1447–1464
30. Baril P et al (2007) Periostin promotes invasiveness and resistance of pancreatic cancer cells to hypoxia-induced cell death: role of the beta4 integrin and the PI3k pathway. Oncogene 26(14):2082–2094
31. Bao S et al (2004) Periostin potently promotes metastatic growth of colon cancer by augmenting cell survival via the Akt/PKB pathway. Cancer Cell 5(4):329–339
32. Kanno A et al (2008) Periostin, secreted from stromal cells, has biphasic effect on cell migration and correlates with the epithelial to mesenchymal transition of human pancreatic cancer cells. Int J Cancer 122(12):2707–2718
33. Tischler V et al (2010) Periostin is up-regulated in high grade and high stage prostate cancer. BMC Cancer 10:273
34. Kudo Y et al (2006) Periostin promotes invasion and anchorage-independent growth in the metastatic process of head and neck cancer. Cancer Res 66(14):6928–6935

35. Puppin C et al (2008) High periostin expression correlates with aggressiveness in papillary thyroid carcinomas. J Endocrinol 197(2):401–408
36. Soltermann A et al (2008) Prognostic significance of epithelial-mesenchymal and mesenchymal-epithelial transition protein expression in non-small cell lung cancer. Clin Cancer Res 14(22):7430–7437
37. Puglisi F et al (2008) Expression of periostin in human breast cancer. J Clin Pathol 61(4):494–498
38. Song LB et al (2002) Molecular mechanisms of tumorigenesis and metastasis in nasopharyngeal carcinoma cell sublines. Ai Zheng 21(2):158–162
39. Cheung HW et al (2005) Mitotic arrest deficient 2 expression induces chemosensitization to a DNA-damaging agent, cisplatin, in nasopharyngeal carcinoma cells. Cancer Res 65(4):1450–1458
40. Cheng AL et al (2008) Identificating cathepsin D as a biomarker for differentiation and prognosis of nasopharyngeal carcinoma by laser capture microdissection and proteomic analysis. J Proteome Res 7(6):2415–2426
41. Hermani A et al (2005) Calcium-binding proteins S100A8 and S100A9 as novel diagnostic markers in human prostate cancer. Clin Cancer Res 11(14):5146–5152
42. Li MX et al (2009) Quantitative proteomic analysis of differential proteins in the stroma of nasopharyngeal carcinoma and normal nasopharyngeal epithelial tissue. J Cell Biochem 106(4):570–579
43. Thompson CC et al (2007) Pancreatic cancer cells overexpress gelsolin family-capping proteins, which contribute to their cell motility. Gut 56(1):95–106
44. Nomura H et al (2008) Clinical significance of gelsolin-like actin-capping protein expression in oral carcinogenesis: an immunohistochemical study of premalignant and malignant lesions of the oral cavity. BMC Cancer 8:39
45. Li MX et al (2010) Proteomic analysis of the stroma-related proteins in nasopharyngeal carcinoma and normal nasopharyngeal epithelial tissues. Med Oncol 27(1):134–144
46. Kim SH et al (2011) Nuclear localization of Nm23-H1 in head and neck squamous cell carcinoma is associated with radiation resistance. Cancer 117(9):1864–1873
47. Wu M et al (2009) Signaling transduction network mediated by tumor suppressor/susceptibility genes in NPC. Curr Genomics 10(4):216–222
48. Kikuchi Y et al (2008) Periostin is expressed in pericryptal fibroblasts and cancer-associated fibroblasts in the colon. J Histochem Cytochem 56(8):753–764
49. Chen ZG (2007) Exploration of metastasis-related proteins as biomarkers and therapeutic targets in the treatment of head and neck cancer. Curr Cancer Drug Targets 7(7):613–622
50. Siriwardena BS et al (2006) Periostin is frequently overexpressed and enhances invasion and angiogenesis in oral cancer. Br J Cancer 95(10):1396–1403